FINITE ELEMENT ANALYSIS OF CRACK INITIATION IN PARTIALLY ELECTRODED PZT TRANSDUCERS

Radim Dolezal, Josef Novak

Technical University of Liberec,
Faculty of Mechatronics and Interdisciplinary Engineering Studies,
Halkova 6, 461 17 Liberec, Czech Republic

josef.novak@tul.cz (Josef Novak)

Abstract

Piezoelectric transducers have been used in wide applications range. The transducers frequently fracture under high electric fields in many applications. The most efficient geometry for some transducers has the disadvantage of electrodes ending inside the ceramic. There are maximum magnitudes of electric field on the electrodes boundary and it cause a stresss concentration. A stress concentration due to boundary of electroded and nonelectroded parts is the consequence. High mechanical stresses at these regions lead to crack initiation and crack propagation and finally to the fault of the transducer. An initiation of cracks by stress concentration during the first poling cycle in partially electroded PZT's is investigated. There was chosen a circular partially electrode specimen. The focus is laid on the electrode shape and placement influence to crack initiation. The most interesting part is optimization of electrode shape to minimizing a stress concentration. Mathematical analysis of electric and elastic fields is very efficient tool for improvement of parameters of piezoelectric transducers. This work is based on finite element method, possibilities of ANSYS package are used. Our results show, that the proportions of electrodes are very important parameters of partially electroded transducers. Important parameters are placement of electrodes and their shape. These results are based only on electric field analysis. Piezoelectric effect and spontaneous deformation are neglected.

Keywords: finite element method, piezoelectric transducers, crack initiation, optimization

Presenting Author's Biography

Josef Novak. He obtained PhD degree in Electrical Engineering from Technical University of Liberec, Czech Republic. He is currently Research and Educational Secretary of Institute of Advanced Technollogies at Technical University of Liberec. His research is focused on modelling of technical processes and systems.

ISBN 978-3-901608-32-2

1 Introduction

Piezoelectric transducers have been used in wide applications range from aircraft and automotive to printers and textile machinery. The transducers frequently fracture under high electric fields. The most efficient geometry for some transducers has the disadvantage of electrodes ending inside the ceramic. There are maximum magnitudes of electric field on the electrodes boundary and it cause a stresss concentration. A stress concentration due to boundary of electroded and nonelectroded parts is the consequence. High mechanical stresses at these regions lead to crack initiation and crack propagation and finally to the fault of the transducer.

An initiation of cracks by stress concentration during the first poling cycle in partially electroded PZT's is investigated. There was chosen a circular partially electrode specimen. The focus is laid on the electrode shape and placement influence to crack initiation. The most interesting part is optimization of electrode shape to minimizing a stress concentration.

Design and improvement of piezoelectric transducers is very complicated process, which is not able without mathematical-physical models. Mathematical analysis of electric and elastic fields is very efficient tool for improvement of parameters of piezoelectric transducers.

There were published some papers related this problem in the last years. Model based on finite difference method is described in [1], finite element method approach is published in [2], [3]. The foregoing work are [4], [9]. There are shown distributions of electric and elastic fields in transducers and prediction of crack regions.

This work is also based on finite element method, but possibilities of ANSYS package are used. There were also published some papers related to crack initiation and propagation, e.g. [5], [6].

2 Physical description of piezoelectric continuum

There are two differential equations governing the behavior of a piezoelectric continuum - the quasistatic approximation Maxwell's equation and Newton's law of motion, see [7]. Let $\Omega \subset R^3$ is continuous area. Let the boundary Ω is denoted as Γ.

Electric field is described by Maxwell's equation

$$\nabla \cdot \mathbf{D} = \frac{\partial \mathrm{D_i}}{\partial x_i} = 0, \quad \text{on } \Omega \quad i = 1,2,3, \qquad (1)$$

where $\mathbf{D}$ is elecric displacement.

Let the boundary of Ω consist of two disjoint subsets $\Gamma = \Gamma_1 \bigcup \Gamma_2$. There are stated Dirichlet's boundary conditions on Γ_1 (denoted with subscript D) and Neumann's boundary conditions on Γ_2 (denoted with subscript N),

$$\varphi = \varphi_D \quad \text{on} \quad \Gamma_1, \qquad (2)$$
$$\mathrm{D_k} n_k = \mathrm{D_N} \quad \text{on} \quad \Gamma_2., \qquad (3)$$

φ is electric potential.

Elastic field is described by the Newton's law of motion

$$\nabla \cdot \mathbf{T} = \frac{\partial \mathrm{T_{ij}}}{\partial x_j} = 0 \qquad \text{on } \Omega, \quad i = 1,2,3, \quad (4)$$

where $\mathbf{T}$ is stress tensor. There are stated Dirichlet's boundary conditions on Γ_1 (denoted with subscript D) and Neumann's boundary conditions on Γ_2 (denoted with subscript N).

$$u_i = u_{iD} \qquad i = 1,2,3 \qquad \text{on} \quad \Gamma_1, \quad (5)$$
$$\mathrm{T_{ij}} n_j = t_{iN} \qquad i = 1,2,3 \qquad \text{on} \quad \Gamma_2, \quad (6)$$

where u is mechanical displacement.

Description of piezoelectric continuum includes piezoelectric state equations

$$T_{ij} = c_{ijkl} S_{kl} - e_{kij} E_k, \qquad (7)$$
$$D_i = e_{ijk} S_{jk} + \varepsilon_{ij} E_j, \qquad (8)$$

where $\mathbf{c}$, $\mathbf{e}$ and ε are the stiffness, piezoelectric and permitivity tensors. There are constitutive equations between electric field $\mathbf{E}$ and potential φ, strain tensor $\mathbf{S}$ and displacements $\mathbf{u}$

$$\mathrm{S}_{ij} = \frac{1}{2}\left[\frac{\partial u_i}{\partial x_j} + \frac{\partial u_j}{\partial x_i}\right] \qquad i,j = 1,2,3,$$
$$\mathrm{E_k} = \frac{\partial \varphi}{\partial x_k} \qquad k = 1,2,3.$$

Now, we can fulfill previous constitutive equations and piezoelectric state equations into equations (1), (4)

$$\nabla \cdot \mathbf{D} = \frac{\partial}{\partial x_k}\left(e_{kij} \cdot \frac{1}{2}\left(\frac{\partial u_i}{\partial x_j} + \frac{\partial u_j}{\partial x_i}\right) - \varepsilon_{kj} \cdot \frac{\partial \varphi}{\partial x_j}\right) = 0, \qquad (9)$$

$$\nabla \cdot \mathbf{T} = \frac{\partial}{\partial x_j}\left(c_{ijkl} \cdot \frac{1}{2}\left(\frac{\partial u_k}{\partial x_l} + \frac{\partial u_l}{\partial x_k}\right) + e_{kij} \cdot \frac{\partial \varphi}{\partial x_k}\right) = 0. \qquad (10)$$

FEM formulation of this problem is included e.g. in [4]. It is not necessary to show FEM formulation here, because we do not implement our own FEM system. ANSYS is used for modelling and ANSYS features are very well known and are described e.g. in ANSYS, Inc. Theory Reference, see [8].

3 Model Preparation

All computations were performed on a model of commercially available transducer produced by Piezoceram

s.r.o., Czech Republic. The transducer is depicted in Fig. 1. A bottom electrode covers whole botom side and it is wrapped on the upper side. The dimensions of specimen are in the Table 1. The scheme of the dimensions is depicted in Fig. 2. The poling electric field during the first poling cycle is 3kV.

Fig. 1 Piezoelectric transducer.

parameter	value
Diameter of transducer D [mm]	19
Radius of wrapped electrode R_1 [mm]	4.2
Radius to upper electrode R_2 [mm]	5.6
Distance from wrapped to upper electrode t [mm]	1.4
Distance from the center of the specimen to wrapping T_s [mm]	3.9
Thickness of transducer h [mm]	1.9

Tab. 1 Parameters of transducer.

Material properties of the transducer are defined by tensors of elastic coefficients s , piezoelectric moduli e and relative permitivity ε,

$$s = \begin{pmatrix} 11.2 & -4.7 & -5.2 & 0 & 0 & 0 \\ -4.7 & 11.2 & -5.2 & 0 & 0 & 0 \\ -5.2 & -5.2 & 15.9 & 0 & 0 & 0 \\ 0 & 0 & 0 & 38.5 & 0 & 0 \\ 0 & 0 & 0 & 0 & 38.5 & 0 \\ 0 & 0 & 0 & 0 & 0 & 33.2 \end{pmatrix} \cdot 10^{-12}(m^2N^{-1}),$$

$$e = \begin{pmatrix} 0 & 0 & 0 & 0 & 12.3 & 0 \\ 0 & 0 & 0 & 12.3 & 0 & 0 \\ -5.4 & -5.4 & 15.8 & 0 & 0 & 0 \end{pmatrix} (Vm^{-1}),$$

$$\varepsilon = \begin{pmatrix} 1730 & 0 & 0 \\ 0 & 1730 & 0 \\ 0 & 0 & 1700 \end{pmatrix}.$$

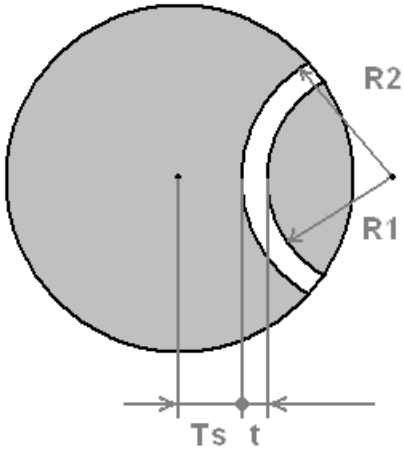

Fig. 2 Scheme of dimensions.

3.1 Finite element model

The model is based on the modelling of spatial distribution of electric field. Piezoelectric effect and spontaneous deformation are neglected. There is used SOLID122 element. SOLID122 is a 3-D, 20-node, charge-based electric element. The element has one degree of freedom, voltage, at each node. It can tolerate irregular shapes without much loss of accuracy. SOLID122 elements have compatible voltage shapes and are well suited to model curved boundaries.This element is applicable to 3-D electrostatic and time-harmonic quasistatic electric field analyses. See SOLID122 in the ANSYS, Inc. Theory Reference [8], for more details about this element.

We consider only one half of the transducer in regard to axis symmetry of transducer. The plane of symmetry is marked in the Fig. 3.

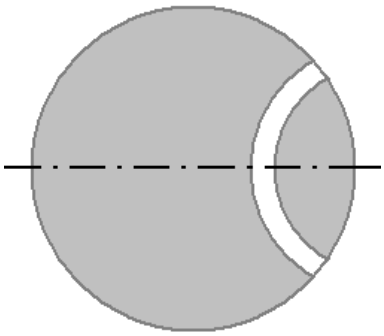

Fig. 3 Plane of transducer's symmetry.

The finite element mesh is slightly finer and mapped around the wrapped electrode. There are evident boundaries between electroded and nonelectroded parts in the mesh. The FE mesh is depicted in Fig. 4.

The electrodes were implemented by coupling the voltage degree of freedom of the surface nodes of electrodes. The voltage 0V is stated on the bottom wrapped electrode and 3kV is stated on the upper electrode.

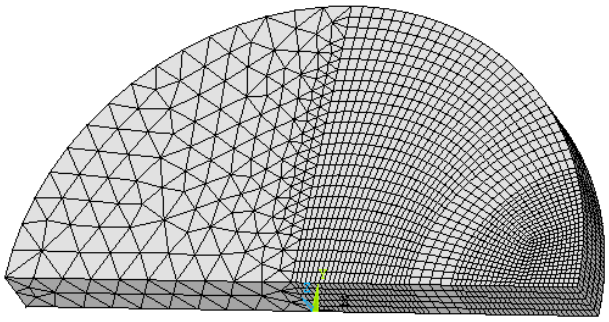

Fig. 4 Finite element mesh of the transducer.

There are Neumann's boundary conditions $\mathbf{D} \cdot n = D_N = 0$ (zero normal components of electric displacement) on the rest of the boundary. We can use homogenous Neuman's boundary condition due to high permitivitty of piezoelectric ceramic.

3.2 Results

Distribution of magnitudes of electric field in the transducer is depicted in Fig. 5.

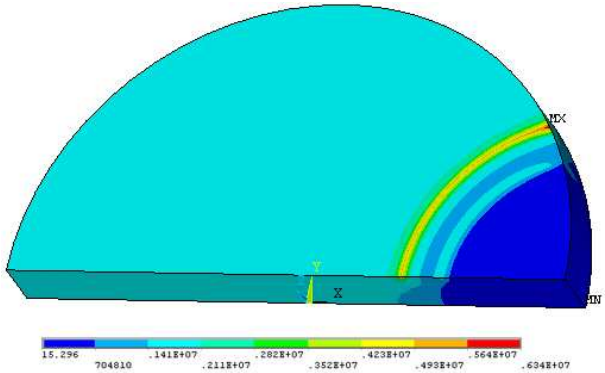

Fig. 5 Distribution of electric field.

The smallest magnitudes are in the wrapped region, between lower and upper part of the bottom electrode. The largest magnitudes are along the upper electrode boundary. This boundary is critical region for crack initiation. The detail view of electric field magnitudes is in the Fig. 6.

There are electric field magnitudes along the line bounding the upper electrode depicted. The bounding line is highlited in the Fig. 7. Maximum magnitude of electric field is $|E_{max}| = 6.34 \cdot 10^6 V \cdot m^{-1}$.

The magnitudes of electric field grow from the centre of the transducer to its boundary and extreme values are on the boundary of the transducer. Minimization of these extreme valus is the goal of the next section.

4 Optimization

Optimization methods are traditional techniques that strive for minimization of a single function subject to constraints. While working towards an optimum design, the ANSYS optimization routines employ three types of variables that characterize the design process: design variables, state variables, and the objective function. These variables are represented by scalar parameters in ANSYS Parametric Design Language (APDL). The state variables can also be referred to as dependent variables in that they vary with the vector x of design variables. The objective function is the function which is optimized. ANSYS optimization features are very well are described in ANSYS, Inc. Theory Reference, see [8].

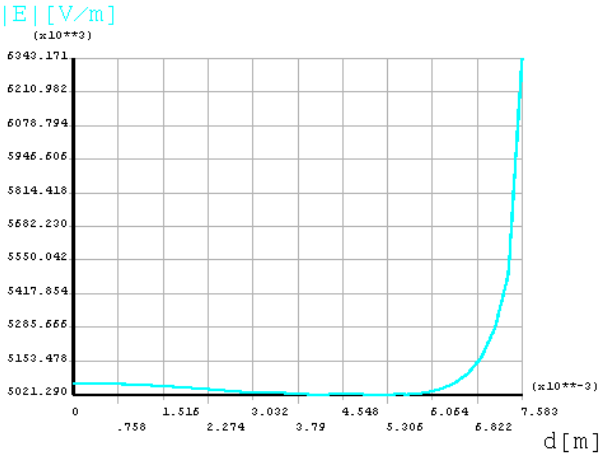

Fig. 6 Magnitudes of electric field along the upper electrode.

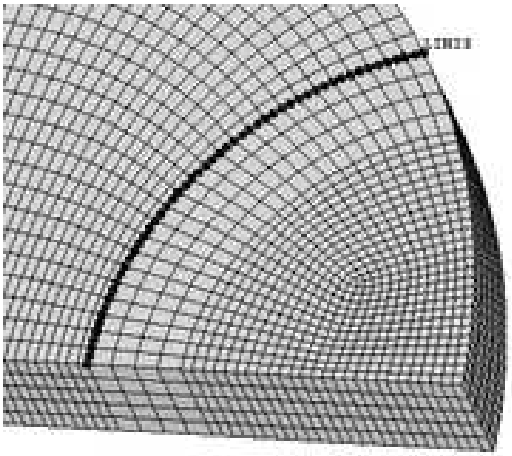

Fig. 7 Bounding line along the upper electrode.

Our main task is to minimize the extreme magnitudes of electric field along the bounding line. One of the possible ways is optimization of shape of electrode's wrapping. The idea is to change radiuses R_1 and R_2 and observe the extreme values $|E_{ex}|$ of electric field magnitudes. We have two design variables (R_1, R_2) and one objective function ($|E_{ex}|$) for optimization. Remaining variables D, T_s, t, h are constant.

In the ANSYS program, several different optimization tools and methods are available. Our optimization pro-

ISBN 978-3-901608-32-2

cedure contains two optimization steps. First step is performed by the Random Design Generation Method and the second step is performed by the First Order Method.

Multiple loops are performed in Random Design Generation, with random design variable values at each loop. A maximum number of loops and a desired number of feasible loops can be specified. This tool is useful for studying the overall design space, and for establishing feasible design sets for subsequent optimization analysis.

First Order Method uses derivative information, that is, gradients of the dependent variables with respect to the design variables. It is highly accurate and works well for problems having dependent variables that vary widely over a large range of design space. However, this method can be computationally intense.

The optimization strategy is: the first step finds solution approximately, the second one gives us more accurate solution. First step (Random Design Generation) contains 25 loops. It is sufficient number of loops for our problem.

4.1 Results

The course of the objective function (electric field magnitude) dependent on design variable R_1 is depicted in Fig. 8.

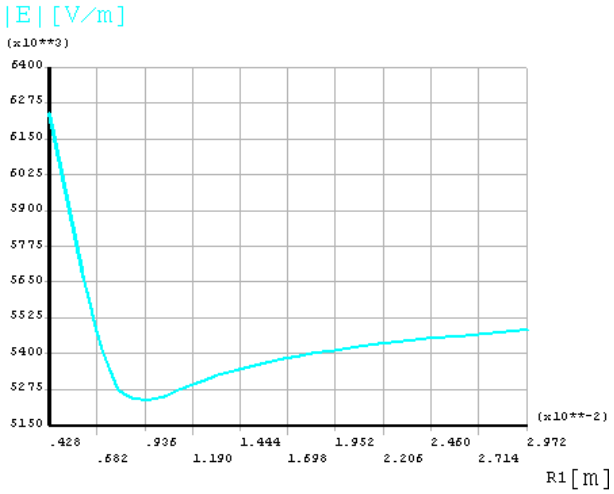

Fig. 8 Dependency of $|E_{ex}|$ on R_1.

Optimal values of design variables are $R_1 = 9.46mm$, $R_2 = 10.86mm$. These values guarantee the minimal values of electric field magnitudes in the transducer. Magnitudes of electric field along the bounding line are depicted in Fig. 9.

Maximum magnitude of electric field after optimization is $|E_{omax}| = 5.21 \cdot 10^6 V \cdot m^{-1}$. This value is much lower than original value.

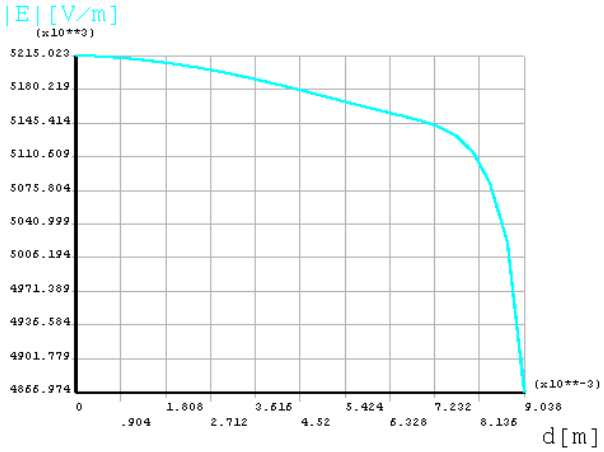

Fig. 9 $|E_{ex}|$ along the bounding line.

5 Conclusion

We can compare maximum magnitudes of electric field before and after optimization. The difference between these values is approx. 18%. Lower values of electric field reduce risk of crack initiation during the first poling cycle in partially electroded PZT transducers. Our results show, that the proportions of electrodes are very important parameters of partially electroded transducers. Important parameter is not only placement of electrodes, important is also their shape.

These results are based only on electric field analysis. Piezoelectric effect and spontaneous deformation are neglected. The effect of spontaneous deformation on crack initiation is described in [4] and [9], but without transducer's optimization.

The optimization procedure including these effects is the main goal of future work. It seems, the magnitude of poling field and no less its direction are important, because of anisotropy of piezoelectric materials.

Acknowledgements:

This project was supplied with the subvention from Czech Science Foundation under Contract Code 102/06/P031.

6 References

[1] Ricinschi D., Ishibashi Y., Okuyama M., Electrostatic Model for the Dielectric Permitivity of Ferroelectric Films with 90^0 Domain Structures, *Jpn. J. Appl. Phys.* Vol. 42, 2003, 6183-6187 .

[2] Th. Steinkopff, Micromechanical Modeling of Ferroelasticity and Ferroelectricity and Finite-Element Results for Nonlinear Piezoelectric Applications, *Ferroelectrics*, Vol. 222, 1999, 126-129 .

[3] S. Kovalev, M. Sakai, Numerical Modeling of Electro-Elastic Field in Ferroelectric Crystal Containing 90^0 Twin Boundary, *Acta mater.*, Vol. 46, 1998, 3015-3026.

[4] J. Novak, J. Maryska, Modelling of Electric and Elastic Fields in Piezoelectric Transducers, Proceedings of ASM 2006, Rhodos, Greece, 2006.

[5] S.L. dos Santos e Lucato, D.C. Lupascu, J. Rodel, Crack initiation and crack propagation in partially electroded PZT, Journal of the European Ceramic Society 21, 2001, 1425-1428.

[6] W. Chen, C.S. Lynch, Finite element analysis of cracksin ferroelectric ceramic materials, Engineering Fracture Mechanics 64, 1999, 539-562.

[7] Milsom R. F., Elliot D. T., Terry Wood S., Redwood M., Analysis and Design of Couple Mode Miniature Bar Resonator and Monolithic Filters, *IEEE Trans Son. Ultrason.*, Vol. 30, 1983, 140-155.

[8] ANSYS Inc., Release 10.0 Documentation for ANSYS, 2005 SAS IP.

[9] J. Novak, Application of FEM in Problems of Piezoelectric and Ferroelectric Structures, *Ph.D. thesis*, Technical University of Liberec, 2004.

ISBN 978-3-901608-32-2